EXPERT REVIEW

Molecular imaging in atherosclerosis

Ali Bassir[1] · William Y. Raynor[1] · Peter Sang Uk Park[1,2] · Thomas J. Werner[1] · Abass Alavi[1] ·
Mona-Elisabeth Revheim[1,3,4]

Abstract

Purpose As atherosclerosis is a prominent cause of morbidity and mortality, early detection of atherosclerotic plaques is vital to prevent complications. Imaging plays a significant role in this goal. Molecular imaging and structural imaging detect different phases of atherosclerotic progression. In this review, we explain the relation between these types of imaging with the physiopathology of plaques, along with their advantages and disadvantages. We also discuss in detail the most commonly used positron emission tomography (PET) radiotracers for atherosclerosis imaging.

Method A comprehensive search was conducted to extract articles related to imaging of atherosclerosis in PubMed, Google Scholar, and Web of Science. The obtained papers were reviewed regarding precise relation with our topic. Among the search keywords utilized were "atherosclerosis imaging", "atherosclerosis structural imaging", "atherosclerosis CT scan" "positron emission tomography", "PET imaging", "^{18}F-NaF", "^{18}F-FDG", and "atherosclerosis calcification."

Result Although structural imaging such as computed tomography (CT) offers essential information regarding plaque structure and morphologic features, these modalities can only detect macroscopic alterations that occur later in the disease's progression, when the changes are frequently irreversible. Molecular imaging modalities like PET, on the other hand, have the advantage of detecting microscopic changes and allow us to treat these plaques before irreversible changes occur. The two most commonly used tracers in PET imaging of atherosclerosis are ^{18}F-sodium fluoride (^{18}F-NaF) and ^{18}F-fluorodeoxyglucose (^{18}F-FDG). While there are limitations in the use of ^{18}F-FDG for the detection of atherosclerosis in coronary arteries due to physiological uptake in myocardium and high luminal blood pool activity of ^{18}F-FDG, ^{18}F-NaF PET is less affected and can be utilized to analyze the coronary arteries in addition to the peripheral vasculature.

Conclusion Molecular imaging with PET/CT has become a useful tool in the early detection of atherosclerosis. ^{18}F-NaF PET/CT shows promise in the early global assessment of atherosclerosis, but further prospective studies are needed to confirm its role in this area.

Keywords Atherosclerosis imaging · PET scan · ^{18}F-NaF · ^{18}F-FDG · Global assessment of cardiac disease

✉ Mona-Elisabeth Revheim
mona.elisabeth.revheim@ous-hf.no;
m.e.rootwelt-revheim@medisin.uio.no

1 Department of Radiology, University of Pennsylvania, Philadelphia, PA, USA

2 Perelman School of Medicine at the University of Pennsylvania, Philadelphia, PA, USA

3 Division of Radiology and Nuclear Medicine, Oslo University Hospital, Nydalen, Postbox 4950, 0424 Oslo, Norway

4 Faculty of Medicine, Institute for Clinical Medicine, University of Oslo, Oslo, Norway

Introduction

Epidemiology and risk factors of atherosclerosis

Atherosclerosis is one of the main causes of morbidity and death in the world, and it is a significant contributor to multiple life-threatening and debilitating diseases [1]. Atherosclerosis may lead to ischemic conditions such as myocardial infarction and stroke, accountable for the deaths of an estimated 10 million persons per year [2]. Early diagnosis of atherosclerosis is crucial to reduce the risks of morbidity and mortality. Risk factors such as diabetes, hypertension, hypercholesterolemia, and smoking place individuals at a higher risk of developing atherosclerosis

via vascular endothelium disruption and a cascade of pro-inflammatory responses [3]. Although clinical evaluation of patients with scoring systems such as Framingham Risk Score and Systemic Coronary Risk Evaluation are used to estimate the pre-test likelihood of having atherosclerosis and stress perfusion imaging has a high predictive power of cardiac ischemia, an early diagnosis of atherosclerosis is best achieved by direct imaging of atherosclerosis.

The biological sequence of atherosclerosis

The biologic sequence of atherosclerosis consists of three pathologic stages: (1) formation of atherosclerotic plaque, (2) progression of plaque, and (3) rupture of plaque. Understanding these stages is necessary for comprehending the ability of specific imaging in detecting each stage. The first stage starts with endothelial dysfunction and inflammation, which causes the buildup of low-density lipoprotein (LDL) in the intima (fatty streak). LDL undergoes oxidative changes in the intima by reactive oxygen species. Modified LDL increases the recruitment of monocytes to the intima. Monocytes develop into macrophages, and with phagocytosis of oxidized lipoprotein, form foam cells. The second stage of plaque progression follows as oxidized lipoprotein is detrimental to macrophages and leads to foam cell death and the development of a necrotic core. With migration of smooth muscle cells from media to intima, a fibrous-cap forms. In the next step, microcalcifications on the fibrous cap appear, which are calcifications with a size of less than 50 μm. The third stage is rupture of the plaque which includes rupture of the fibrous cap, release of the necrotic core in blood, activation of platelets, and thrombus formation [4–6]. It has been shown that several features of atherosclerotic plaques make them vulnerable to rupture. Some prominent features are a thin fibrous cap with a massive lipid core, fissured cap, severe inflammation in the adjacent area of cap, low smooth muscle cell and collagen, endothelial erosion, microcalcification, and intraplaque hemorrhage [7–9].

After the creation of foam cells, the balance between pro-inflammatory and anti-inflammatory mediators determines the future of atherosclerotic plaque. Pro-inflammatory mediators' dominance leads to cell death and promotes additional inflammation and a large necrotic lipid core generation. As mentioned, it is considered a feature of unstable plaques and can ultimately lead to rupture and cardiovascular events. In contrast, the dominance of anti-inflammatory mediators leads to autophagy and efflux of cholesterol from lesions [10]. The plaque may be stabilized as the calcification phase progresses to macrocalcification [11].

Treatment of atherosclerosis

Since atherosclerotic disease is a significant etiology of cardiovascular disease (CVD), plaque regression has been considered a critical approach for treating atherosclerosis. Studies have shown that treatment with statins reduces atheroma size, slows the progression of plaque, diminishes the necrotic core size, decreases total lipid content, reduces inflammation and oxidation [12]. The observed effect meets the criteria suggested for plaque stabilization. As the efficacy of treatment is evident in the stabilization of atherosclerotic plaque, it is necessary to detect atherosclerotic plaques in early stages and prevent complications related to advanced plaques. Advanced atherosclerosis is the principal cause of cardiovascular events and stroke [13, 14]. Hence, prevention of early atherosclerotic plaque progression to advanced plaques is vital to decrease the mortality rate related to CVD. It has been demonstrated that plasma cholesterol-lowering (PCL) drugs, primarily statins, have a significant effect in decreasing progression of atherosclerosis and prevention of cardiovascular events and stroke [15]. Even some degree of regression was observed with high dose statin therapy [16]. An animal study demonstrated that atherosclerosis regression induced by PCL could vary with the lesions' level and magnitude. Complete regression of early lesions and incomplete regression of advanced lesions suggest that if early atherosclerosis is similarly susceptible to plasma cholesterol levels, PCL will significantly help patients at elevated risk of coronary artery disease (CAD) and myocardial infarction (MI) when their lesions are still in the early stage [17]. Therefore, detection of the early atherosclerotic lesion is vital to prevent lesion progression and cardiovascular events.

Calcification in atherosclerosis

Calcification which occurs alongside atherogenesis has become of interest particularly in relation to its ease of detection with imaging. Calcification occurs through several mechanisms, most prominently of which is the death of macrophages and vascular smooth muscle cells (VSMCs), contributing to the eruption of apoptotic bodies and necrotic debris that can act as nuclei for calcification at injury sites [18]. This process arises in response to pro-inflammatory stimuli and leads to the development of microcalcification nuclei, which induces further inflammatory processes and stimulates calcium deposition. This cycle favors the progression of thinning of the fibrous cap, which is a criterion for plaque instability and increases the chance of rupture [19]. However, if inflammation wanes

and VSMCs survive, they can organize an adequately managed mineralization process. This leads to macrocalcification formation, further stabilizing the plaque by serving as a shield to propagate the inflammation (Fig. 1) [11].

Method

A thorough search of PubMed, Google Scholar, and Web of Science from database inception to August 2021 was performed. Search terms used were "atherosclerosis imaging," "atherosclerosis structural imaging," and "atherosclerosis CT scan," "positron emission tomography" and "PET imaging," "18F-NaF", "18F-FDG", and "atherosclerosis calcification." References of extracted articles also were searched for any related articles to the topic. Two researchers independently assessed the articles that had relevant titles or abstracts. Only papers written in English were considered; preprint articles were excluded. Among 345 articles extracted from databases that had the highest number of relevant keywords, 95 articles were selected. There was no statistical analysis done since this was not a systematic review or meta-analysis.

Imaging

Structural imaging

Structural imaging has traditionally played a central role in the diagnosis of atherosclerosis. The development of computed tomography (CT) offered a noninvasive diagnostic imaging option. In the 1980s, the method of measuring the magnitude of the atherosclerotic disease using CT calcification was implemented and standardized with the introduction

of the CT scan calcium score [21]. Recently, other modalities have been used for this purpose, including CT angiography, Magnetic Resonance Imaging (MRI), intravascular ultrasound, and optical coherence imaging [22]. These diagnostic tools provide more information on the plaque structure and morphologic characteristics and risk factors for ruptures, such as a thin fibrous cap, a lipid-rich necrotic core, neovascularization, intraplaque hemorrhage [22]. However, these anatomical imaging modalities can only visualize the macroscopic changes that arise late in the sequence of the disease, when the changes often are irreversible. In the detection of the early stages of atherosclerosis, CT imaging has limited sensitivity as CT imaging cannot differentiate metabolically active atherosclerotic lesions from indolent lesions. CT scan can detect macrocalcification which favors stabilized plaque [23]. However, better resolution of CT scan help in detection of low-density non-calcified plaques, and ultrasound has shown that these plaques are associated with a lipid-rich necrotic core which is considered a feature of unstable plaque [24].

Molecular imaging

Molecular imaging plays a fundamental role in visualizing the early stage of the disease and microscopic change. Positron emission tomography (PET) with 18F-fluorodeoxyglucose (18F-FDG) or 18F-sodium fluoride (18F-NaF) as radiotracers is the most used and studied of these techniques [25]. Tracer uptake is typically calculated as standardized uptake values (SUVs), which describes the ratio of activity per unit volume of a region of interest (ROI) to the activity per unit whole body volume. SUVs are calculated as a maximum value (SUV_{max}) that reflects the highest uptake in a single voxel, or a mean value (SUV_{mean}) that averages all uptake within the ROI. SUV_{mean} is advantageous over
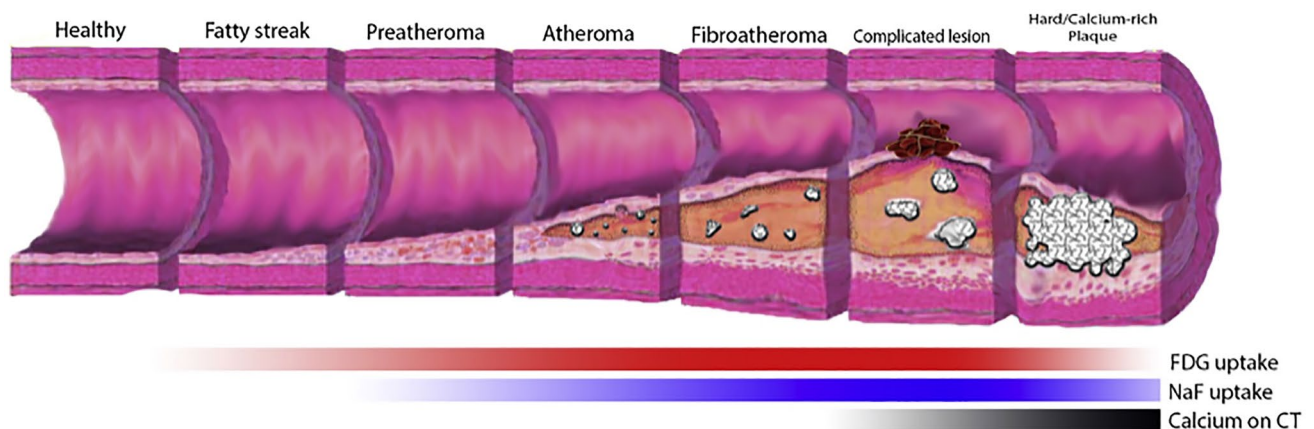

Fig. 1 Progression of a calcium-rich atheroma with the temporal distribution of abnormalities present on 18F-FDG-PET, 18F-NaF-PET, and CT. As a specific marker of active microcalcification, 18F-NaF-PET has great promise in the domain of monitoring atherogenic activity even in early stages of disease. (This figure was reproduced with permission from [20])

SUV_{max}, as SUV_{max} may easily be influenced by the background radiotracer uptake of adjacent tissues or artifacts from motion [26]. Furthermore, focusing only on the region with the highest radiotracer avidity as done by SUV_{max} masks the heterogeneous and diffuse nature of many disease processes [27].

Another commonly used parameter is the target–to–blood pool ratio (TBR), which is calculated by dividing the vascular wall SUV to the venous blood pool SUV to correct for tracer activity in the blood. TBR is often measured using SUV_{max} or SUV_{mean}, resulting in a maximum TBR (TBR_{max}) and mean TBR (TBR_{mean}), respectively [28]. The procedural recommendation of cardiac PET/CT imaging from the European Associating of Nuclear Medicine (EANM) propose quantification of ^{18}F-FDG activity using SUV_{max}, SUV_{peak}, SUV_{mean} and application of TBR analysis [29]. The use of TBR, however, should be approached with caution as it currently stands as a disputed method, as there is no adequate biological explanation for its use [28]. Instead, support for TBR is based on the belief that taking ratio of two measurements will serve as a form of standardization, limiting the effects of differential acquisition time points and accounting for the intrinsic tracer activity [29]. Nevertheless, calculation using the venous blood pool SUV can introduce greater variability because venous blood pool SUV is influenced by numerous factors such as glomerular filtration rate, rate of venous blood flow, and blood cell density [30, 31]. Furthermore, the methodology for measuring venous blood pool SUV itself is wide-ranging, with reports of using various regions such as superior vena cava, inferior vena cava, right atrium, and jugular vein to derive it [28]. Lastly, as venous uptake is often minimal, small variations and measurement errors of the venous blood pool SUV can significantly affect TBR calculation [28]. A study by Johnsrud et al. study showed that quantification methods without background correction had the highest inter-reader agreement for ^{18}F-FDG PET of carotid artery plaque inflammation [32].

The emerging method that overcomes some of the problems imposed by the SUV method for quantifying radiotracer uptake is the global disease assessment (e.g., Alavi-Carlsen

Score). Unlike the focal approach of examining radiotracer uptake in small specific regions such as the coronary arteries, global disease assessment measures diffuse uptake in the entire body, major blood vessels or whole organs such as the aorta and heart that reflects the global burden of the disease [27, 33]. As arteries have small volumes, they are susceptible to the partial volume effect and motion artifacts resulting from respiratory- and cardiac movements that can influence the measures. However, assessment of the overall disease burden may provide more valuable information than a lesion-based approach in risk stratification [34]. Additionally, measurements using easily identifiable and well-defined structures allow for easily replicable approaches analysis amenable to analysis by artificial intelligence [35]. Previous studies have demonstrated the superiority of this approach in measuring CVD burden in various disease conditions such as multiple myeloma and type 2 diabetes [36, 37]. Sorci et al. have additionally shown that in a retrospective analysis of 86 healthy controls and 50 patients, the global disease assessment of ^{18}F-NaF uptake in the whole heart in patients was found to be greater than that of controls and predicted the patient status [38]. As such, the global disease assessment captures the diffuse and systemic nature of vascular disorders such as atherosclerosis and offers a reliable method of quantifying disease burden for clinicians (Table 1).

^{18}F-FDG

^{18}F-FDG is a radiolabeled glucose analog that acts as an indicator for metabolic activity and inflammation. It has been shown that uptake of this marker is highest in macrophages [39]. A study by Ogawa and colleagues has demonstrated that aggregation of ^{18}F-FDG during foam cell development was increased. Still, after the cells had fully differentiated into foam cells, uptake was reduced to the control level. These results indicate that in atherosclerosis, ^{18}F-FDG PET detects the early step of foam cell development. They also demonstrated an association of ^{18}F-FDG uptake with hexokinase activity [40]. Furthermore, macrophages significantly contribute to the formation of plaque inflammation,

Table 1 Comparison between structural and molecular imaging

	Structural imaging	Molecular imaging
Advantages	Offers greater information about the structure and morphology of the plaque, as well as the risk factors for ruptures Higher-resolution aids in the diagnosis of low-density, non-calcified plaques	Detects microscopic changes early in the disease's course when progression can be suppressed Can detect metabolic activity within plaque to differentiate between active and indolent plaque
Disadvantages	Visualizes the macroscopic alterations that occur late in the disease's course, when the effects are frequently permanent Inability to distinguish between metabolically active and indolent atherosclerotic lesions	Small plaque may not be detectable due to limited spatial resolution Cardiac and respiratory movements decrease the quality of images

and it has been reported that ruptured plaques contain large amounts of macrophages [41, 42]. Consequently, the observation that the absorption of ^{18}F-FDG is directly proportional to macrophage density shows the effectiveness of ^{18}F-FDG for plaque susceptibility evaluation [43]. Since inflammatory cells use significant quantities of glucose in contrast to other plaque cells, ^{18}F-FDG PET imaging may indicate inflammatory activities in atherosclerosis, which potentially aids the detection of unstable plaque [44].

Multiple studies demonstrated an association between ^{18}F-FDG uptake and cardiovascular risk factors such as hypertension and hypercholesterolemia [45, 46]. It is also demonstrated that ^{18}F-FDG uptake increases with aging [47]. In a study by Tahara et al., after assessment of 216 patients who underwent ^{18}F-FDG PET scan for cancer screening, they found significant correlations between SUVs of ^{18}F-FDG and body mass index (BMI), waist circumference, carotid intima-media thickness (IMT) ($p < 0.001$), systolic blood pressure, HDL cholesterol (inversely), Homeostatic Model Assessment for Insulin Resistance (HOMA-IR), uric acid, hs-CRP, and medication for hypertension. There was a positive association between metabolic syndrome elements and ^{18}F-FDG uptake due to carotid atherosclerosis. The most significant of these elements were waist circumference and HOMA-IR [48]. Another study by Wassélius and colleagues in 200 patients showed a similar finding. They found a higher quantity of cardiovascular risk factors correlate with the number of plaques with enhanced ^{18}F-FDG uptake [49]. Several studies have reported a relation between ^{18}F-FDG uptake and cardiovascular events. A survey by Paulmier et al. showed that previous cardiovascular events (> 6 months before or after PET) and current cardiovascular events (< 6 months before or after PET) were meaningfully more common in the high ^{18}F-FDG uptake vs. the low ^{18}F-FDG uptake group (48% vs. 15%, respectively ($p < 0.0006$),

and 30% vs. 1.8%, respectively ($p < 0.0002$)). They concluded that extensive elevated vascular absorption of ^{18}F-FDG tends to indicate an emerging atherosclerotic process and the possibility of future cardiovascular incidents [50].

The relation between tracer uptake and CT scan calcification is an area of interest. It has consistently been shown that the correlation between ^{18}F-FDG and the more traditional CT calcification diagnostic method is very poor [46, 51, 52]. Such studies imply that inflammation and macrocalcification are two distinct phases.

[18]F-NaF

[18]F-NaF has been conventionally used for skeletal imaging as a marker of bone mineralization. This tracer's mechanism consists of an exchange process with hydroxyl groups, in which the [18]F$^-$ ion is incorporated directly into the exposed hydroxyapatite crystal [53]. Therefore, it can detect areas of calcification and ossification in the body, and it is used to detect primary and metastatic bone disease [54, 55]. As the pathophysiology of atherosclerosis contains calcification, the mechanism of ^{18}F-NaF has drawn the attention of scientists to use it as an indicator for the detection of atherosclerosis. Creager et al. found that ^{18}F-NaF had a stronger affinity for hydroxyapatite when compared to other significant biological calcium salts. The ^{18}F-NaF ligand binds to the calcification's surface, and the microcalcifications with larger surface area result in better absorption. For macrocalcifications, on the other hand, the radioactivity signal is substantially lower [56]. Therefore, the specificity of ^{18}F-NaF for microcalcification suggests this tracer for detecting atherosclerosis plaque in the early stage (Fig. 2).

Association between the cardiovascular risk factor and ^{18}F-NaF uptake can determine this imaging's efficacy in screening high-risk patients (Fig. 3). Oliveira-Santos et al.

Fig. 2 The hypothesized trends of ^{18}F-FDG uptake, ^{18}F-NaF uptake, and CT calcification in the arterial wall with aging. Uptake of ^{18}F-NaF appears to be more persistent compared to that of ^{18}F-FDG, which increases and decreases with damage to the arterial wall. Once macrocalcifications have become sufficiently stable in later years of life, ^{18}F-NaF uptake may decrease while there is stronger evidence of CT calcification. (This figure was reproduced with permission from [57])
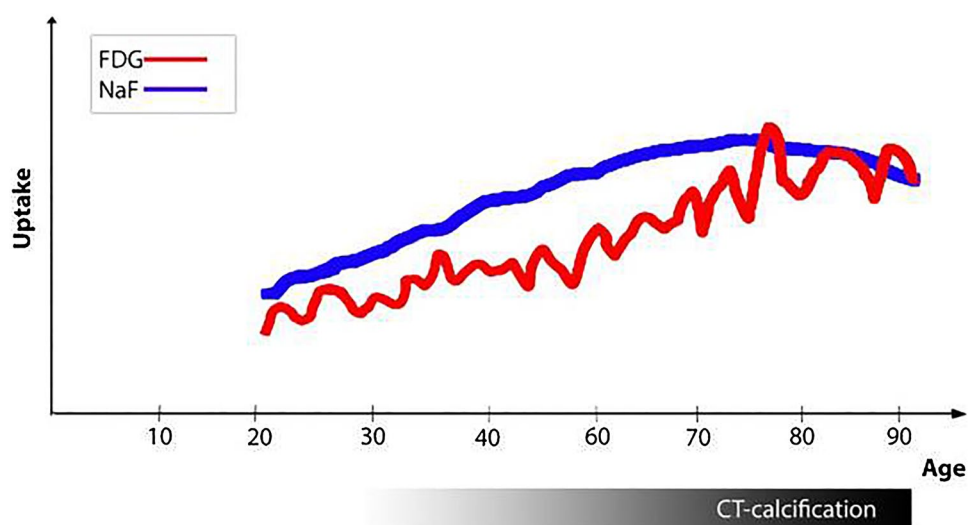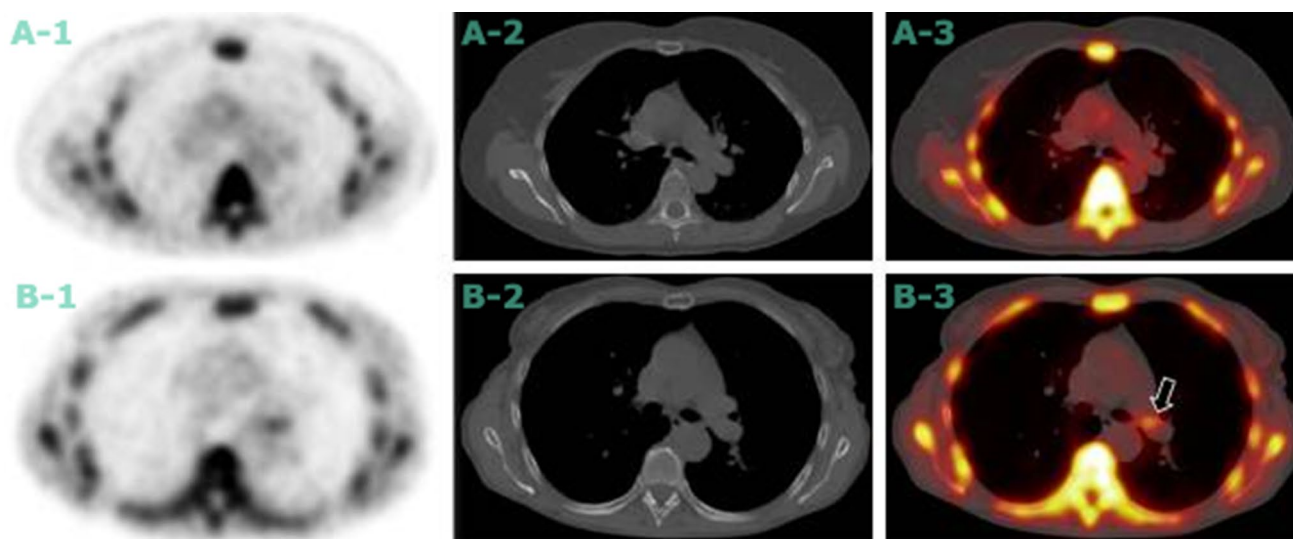
Fig. 3 Axial PET scan (A-1 and B-1), Axial CT scan (A-2 and B-2), and axial fused scan (A-3 and B-3) of pulmonary artery. ^{18}F-NaF PET/CT image showing no focal uptake at the pulmonary artery in (A series) a healthy 62-year-old female. By contrast, focal ^{18}F-NaF avidity is appreciated in the pulmonary artery (black arrow) in (B series) a 63-year-old female with angina pectoris. (This figure was reproduced with permission from [60])

evaluated the proportion of ^{18}F-NaF positive coronary, aortic, and carotidal plaques in high cardiovascular (CV) risk subjects and their relationship to conventional CV risk factors, coronary artery calcium score, and thoracic fat volume. They found that individuals having five or more risk factors had a higher corrected uptake per lesion (CUL: the difference between the lesion and superior vena cava SUV) than those with fewer risk factors (1.1 ± 0.3 vs. 0.7 ± 0.3, $p < 0.01$) [58]. In a study by Rojulpote et al., the authors found that ^{18}F-NaF PET/CT was able to detect a heavier burden of widespread coronary microcalcification in a subgroup with higher blood pressures in asymptomatic individuals without a documented diagnosis of hypertension and the absence of other risk factors such as diabetes, dyslipidemia, smoking, and systemic inflammatory state (0.62 ± 0.043 non-hypertensive group vs. 0.71 ± 0.04 hypertensive group, $p = 0.0006$)[59]. A key point to consider is that the investigators measured coronary artery uptake with the ROI delineating individual arteries in the former study. This approach has limitations because of the PET imaging obstacles which are mentioned. By contrast, global assessment consisting of an ROI encompassing all coronary arteries may be a better approach also used in the latter study. Besides that, individual measurements of diastolic blood pressure (DBP) and mean arterial pressure (MAP) were found to correlate positively with the magnitude of global coronary atherosclerosis as calculated by ^{18}F-NaF PET/CT (DBP ($r = 0.64$, $p = 0.002$), and MAP ($r = 0.59$, p = 0.007)) [59].

Association between ^{18}F-NaF uptake and cardiovascular events is essential for predicting this tracer's role for future morbidity and mortality. Kwiecinski et al. evaluated the role

of ^{18}F-NaF in the prediction of myocardial infarction in a study of patients with established advanced CVD. It was demonstrated that only patients with elevated coronary ^{18}F-NaF uptake (20 of 203 with a cardiac metabolic activity (CMA) > 0 vs. 0 of 90 with a CMA of 0; $p < 0.001$) experienced fatal or nonfatal myocardial infarction. Regardless of age, sex, risk factors, segment involvement, coronary calcium scores, and prior myocardial infarction, patients with CMA > 1.56 had a more than sevenfold rise in lethal or non-lethal MI (hazard ratio: 7.1, $p = 0.003$) [61]. In another study, Kitagawa and colleagues included individuals with known or suspected CAD with coronary computed tomography angiography (CCTA). Patients with at least one coronary atherosclerotic lesion underwent ^{18}F-NaF PET/CT scan, and they followed up patients for 2 years. When a patient has been diagnosed with many atherosclerotic coronary lesions, for a patient-based assessment, the maximum TBR_{max} per patient(M-TBR_{max}) was determined. M-TBR_{max} was more significant in those who had coronary events than those who did not (1.39 ± 0.18 vs. 1.19 ± 0.17, respectively; $p = 0.0034$) [62]. These studies show the ability of ^{18}F-NaF in the prediction of future cardiovascular events.

The relation between coronary calcium score measured with CT scan and ^{18}F-NaF uptake has been studied (Fig. 4). Oliveira-Santos and colleagues found no relation between calcium score and ^{18}F-NaF uptake in hypertensive patients with cardiovascular risk factors ($p = 0.87$). They concluded that it is possible because these approaches distinguish various pathophysiological stages in the atheroma calcification process [58]. Macrocalcifications detected at CT scans are considered to represent stable areas where the
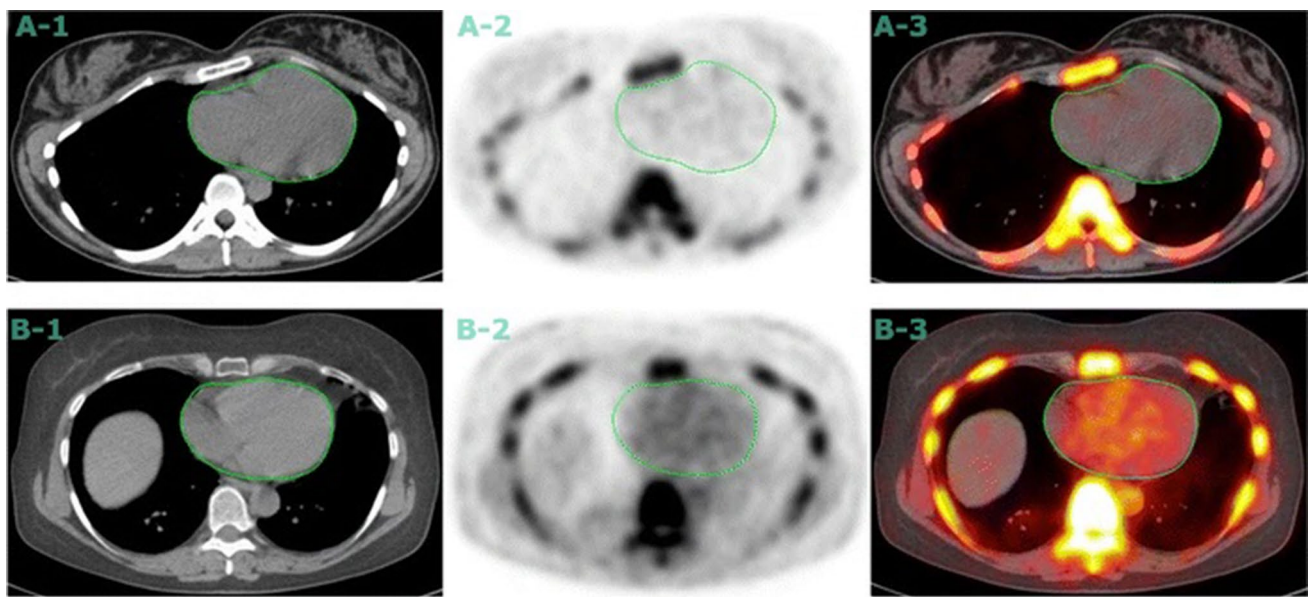
Fig. 4 Axial CT scan (A-1 and B-1), Axial PET scan (A-2 and B-2), and axial fused scan (A-3 and B-3) of two clinically normal subjects (A, 25-year-old) and (B, 61-year-old) with delineating heart. ^{18}F-NaF PET/CT images demonstrating differential coronary ^{18}F-NaF uptake in **A** in comparison with **B**. The matching CT scan shows no structural calcification at the areas of NaF uptake in subject (**B**), and the PET and CT results are significantly different. Coronary calcifica-tion as assessed by CT does not portray the full extent of the disease, as evidenced by its discrepancy with ^{18}F-NaF PET/CT findings. Evidence of molecular changes in the absence of irreversible macrocalci-fication may allow for early interventions that can change the course of the disease. (This figure was reproduced with permission from [64])

atherosclerotic disease is quiescent, whereas the sites with ^{18}F-NaF uptake show active microcalcification believed to represent unstable plaques. Another study by Cecelja et al. showed only a weak link between baseline calcium volume and radiotracer uptake score [63]. They concluded that targeting active calcification by ^{18}F-NaF is the cause of this weak correlation.

One advantage of ^{18}F-NaF is that it is rapidly removed from blood circulation as only 10% of injected tracer remains in blood after 1 hour [65]. This feature leads to the high contrast between the calcification areas and the background activity. Furthermore, the minimal uptake of ^{18}F-NaF by the heart makes it superior in evaluating coronary arteries (Fig. 5) [66]. In a prospective clinical trial by Joshi and colleagues on patients with myocardial infarction and stable angina, the highest coronary ^{18}F-NaF uptake was seen in the culprit plaque in 93% of patients with myocardial infarction (median maximum tissue-to-background ratio: culprit 1.66 (IQR 1.40–2.25) vs. highest non-culprit 1.24 [1.06–1.38], $p < 0.0001$). In contrast, there were no meaningful distinctions between culprit and non-culprit plaques in the study of coronary arteries with ^{18}F-FDG even in visible areas (myocardial uptake frequently masked coronary ^{18}F-FDG uptake) (1.71 (1.40–2.13) vs. 1.58 (1.28–2.01), $p = 0.34$) [66]. This study demonstrated the ability of ^{18}F-NaF in identifying not only ruptured plaque, but also high-risk plaque prone to rupture in the future and causing cardiovascular events. However, it is shown that there is no definitive proof that individual plaque evaluation predicts the likelihood of an acute coronary accident better than proven risk factors like the extent and severity of coronary heart disease [67]. Considering that atherosclerosis is a dynamic process and changes constantly, emphasis on the entire atherosclerosis process and global imaging of the heart stands as a better approach instead of focusing on a single plaque [33, 68]

Other tracers

The study of atherosclerosis plaque by molecular imaging is not limited to only ^{18}F-NaF and ^{18}F-FDG. A study published by Tarkin et al. used gallium-68-labeled DOTA-TATE (^{68}Ga-DOTATATE) to recognize arterial inflammation in macrophages by targeting the somatostatin receptor. Compared to ^{18}F-FDG, it has preferable coronary imaging, superior macrophage specificity, and greater differentiation of high risk vs. low coronary injuries [70]. Kircher and colleagues used chemokine receptor 4 (CXCR4)- directed ^{68}Ga-Pentixafor as a tracer and compared it with ^{18}F-FDG in atherosclerotic lesions. They showed that ^{68}Ga-pentixafor and ^{18}F-FDG absorption had a poor association in lesion-to-lesion comparison ($r = 0.28$; $p < 0.01$). Also, more lesions ($n = 290$; TBR ≥ 1.6, $p < 0.01$) and higher absorption were found by ^{68}Ga-pentixafor PET in comparison with ^{18}F-FDG PET (1.8 ± 0.5 vs. 1.4 ± 0.4; $p < 0.01$) [71]. Mateo et al. used

Fig. 5 Global assessment of ^{18}F-NaF uptake in various arterial vessels in a 67-year-old man. Regions of interest measured activity in the left carotid artery (**A**), coronary arteries (**B**), ascending aorta (**C**), aortic arch (**D**), descending aorta (**E**), abdominal aorta (**F**), bilateral common iliac arteries (**G**), external iliac arteries (**H**), femoral arteries (**I**), and popliteal arteries (**J**) to calculate the Alavi-Carlsen global molecular calcium score, which in this patient was determined to be 16.08. (This figure was reproduced with permission from [69])
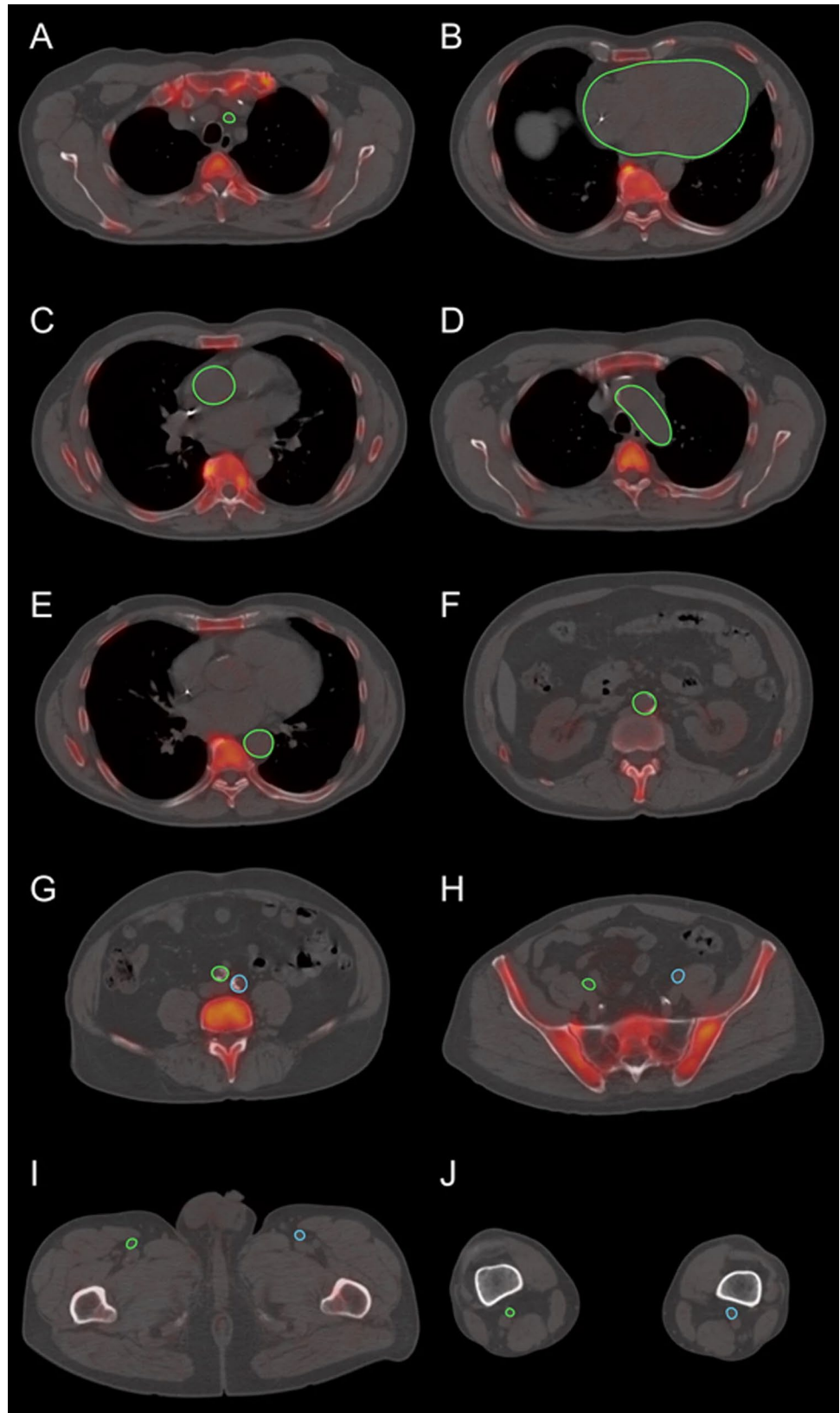
^{18}F-FMISO to detect hypoxia in atherosclerotic plaque in rabbits and found that this tracer has significant uptake in the aortas of atherosclerotic animals and also an increase with atherogenic diet over time [72]. Although these studies provide valuable information regarding atherosclerotic plaque molecular imaging, additional studies are needed to provide more details on the efficacy of these tracers (Fig. 6) (Table 2).

Limitations of PET instruments and PET tracers

Like other imaging modalities, PET imaging is not flawless. For ^{18}F-FDG specifically, its limitations as a probe for atherosclerosis include the nonspecific uptake of ^{18}F-FDG in the arterial wall's smooth muscles and the surrounding tissues. Background ^{18}F-FDG uptake can result from nonspecific inflammation as well (e.g., Takayasu arteritis, chemotherapy, or radiation-induced vascular inflammation), which could obfuscate atherosclerosis evaluation [74]. In addition, the fact that ^{18}F-FDG remains in circulation for an extended period raises concerns regarding the assessment of suspected atherosclerotic plaques [75].

Limitations more general to PET imaging include its limited spatial resolution, which cannot extend to the 5 mm known as mean in phantom studies [76] and remains in the range of 8–10 mm in human study [77]. In the achievement of this range, the function of reconstruction algorithms cannot be ignored. Molecular detection of biological activities needs a large mass of foci accumulated in volumes more than several mm [78]. Atherosclerotic plaques in the major arteries are just a few millimeters wide, even in the advanced phases of the disease. Therefore, they cannot be visualized in vivo with satisfactory sensitivity.

These limitations ultimately contradict the methodology of focally measuring CVD burden by assessing radiotracer uptake in small arteries. Attempts at determining ^{18}F-FDG uptake in the coronary arteries for the detection of atherosclerosis, for instance, are further thwarted by the nonspecific myocardium uptake of ^{18}F-FDG and the constant cardiac and respiratory movements of the heart and diaphragm, respectively [79, 80]. Although the suggested method for resolving these adverse phenomena is cardiac and respiratory gating, the efficacy of such methods can be questionable as respiratory movements are irregular and often significant, extending up to several centimeters [81]. Overall, global disease assessment of the entire body, major vessels, or whole organs such as the aorta or heart using ^{18}F-NaF holds promise for overcoming these limitations and reliably measuring systemic disease burden. Because the use of ^{18}F-NaF PET scan for vascular imaging is new, the current literature
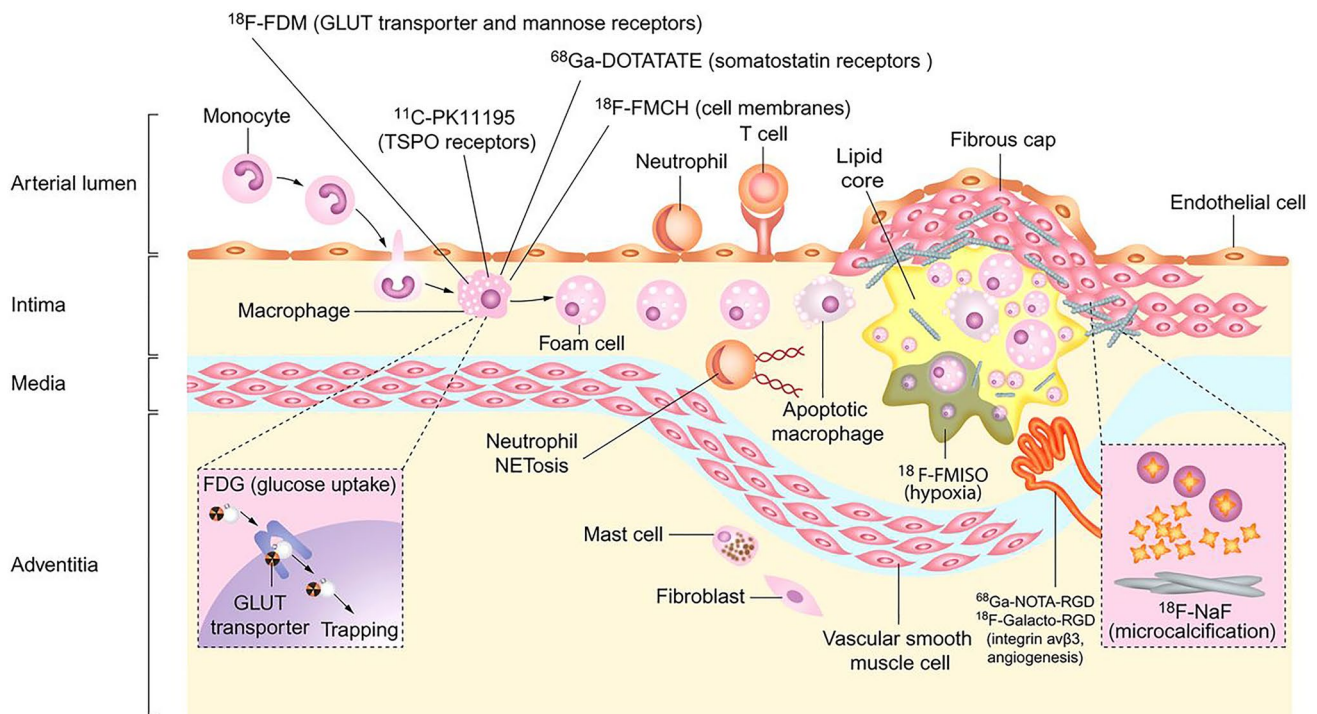

Fig. 6 Cellular targets for PET imaging of atherosclerosis. Macrophage activity is responsible for increased ^{18}F-FDG uptake as a reflection of increased glycolysis. ^{18}F-fluorodeoxymannose, ^{68}Ga-DOTATATE, ^{11}C-PK11195, and ^{18}F-FMCH uptake is also mediated by macrophages. Cellular hypoxia is targeted by ^{18}F-FMISO, while ^{68}Ga-NOTA-RGD and ^{18}F-Galacto-RGD show areas of neoangiogenesis. Microcalcification is uniquely revealed by ^{18}F-NaF activity. (This figure was reproduced with permission [73])

Table 2 Summary of main findings from the reviewed literature for ^{18}F-NaF, ^{18}F-FDG and other tracers in molecular imaging of atherosclerosis

	^{18}F-NaF	^{18}F-FDG	Other tracers
Main findings	The specificity of this tracer for microcalcification suggests it for detection of atherosclerotic plaques early in their development [56, 57] The corrected uptake per lesion (CUL) was higher in people who had five or more CV risk factors[58] In asymptomatic individuals without hypertension and the absence of other risk factors, this tracer was able to detect a higher burden of widespread coronary microcalcification in a subgroup with higher blood pressures [59] Patients with cardiac metabolic activity (CMA) > 1.56 had a more than sevenfold rise in lethal or nonlethal MI [61] In individuals who had coronary incidents, M-TBR$_{max}$ was more significant than in those who had not [62] The baseline calcium volume and radiotracer uptake score have a poor connection due to this tracer targeting active calcification[60, 63] The heart's low absorption of this tracer makes it ideal for assessing coronary arteries [66] This tracer can distinguish between culprit and non-culprit on myocardial infarction and stable angina patients, but ^{18}F-FDG cannot make this distinction [34][34]	Detects the formation of foam cells [34], and the uptake is highest in macrophages [39, 41, 42] Its uptake has an association with hexokinase activity [40] Demonstrate inflammatory activities in atherosclerosis, which helps to detect unstable plaques[43, 44] Its uptake is associated with cardiovascular risk factors such as hypertension and hypercholesterolemia [45, 49], and also metabolic syndrome elements such as waist circumference and HOMA-IR [48] Previous and current cardiovascular events were more common in the high tracer uptake group [50] Correlation between its uptake and the more traditional CT calcification diagnostic method is weak, suggesting that inflammation and macrocalcification are two distinct phases and this tracer detect late stage of atherosclerosis [51, 52] Its uptake increases with aging [47]	^{68}Ga-DOTATATE has desirable coronary imaging, superior macrophage specificity, and greater differentiation of high risk vs. low coronary injuries in comparison with ^{18}F-FDG [70] In comparison to ^{18}F-FDG, ^{68}Ga-pentixafor detected more lesions and higher absorption [71] In rabbits, ^{18}F-FMISO was used to identify hypoxia in atherosclerotic plaque, and it was discovered that this tracer has a large absorption in the aortas of atherosclerotic animals, as well as an increase over time with an atherogenic diet [72]

on ^{18}NaF-PET imaging of atherosclerosis is restricted and lacking in long-term follow-up studies and intervention trials. Further research is required to help scientists for better understanding of strengths and weaknesses of this imaging.

Conclusions

As atherosclerosis is a key cause of morbidity and mortality, imaging plays a substantial role in uncovering mechanisms and monitoring the disease's progression. The detection of atherosclerosis in the early stages while the disease is still treatable is critical. Anatomical imaging mainly detects late stages dormant macrocalcification, but it is the early molecular changes in the atherosclerotic process that is of greater importance. This fact establishes molecular imaging with PET as a unique player in the imaging of atherosclerosis.

Availability of data and materials All of the data used in this study is available in the associated papers.

Code availability Not applicable.

Declarations

Conflict of interest The authors (Ali Bassir, William Y. Raynor, Peter Sang Uk Park, Thomas J. Werner, Abass Alavi, Mona-Elisabeth Revheim) have no financial or proprietary interests in any material discussed in this article.

References

1. Lloyd-Jones D, Adams R, Carnethon M et al (2009) Heart disease and stroke statistics—2009 update. Circulation. https://doi.org/10.1161/circulationaha.108.191261
2. Lozano R, Naghavi M, Foreman K et al (2012) Global and regional mortality from 235 causes of death for 20 age groups in 1990 and 2010: a systematic analysis for the Global Burden of Disease Study 2010. Lancet 380:2095–2128. https://doi.org/10.1016/S0140-6736(12)61728-0
3. Tarkin JM, Joshi FR, Rudd JHF (2014) PET imaging of inflammation in atherosclerosis. Nat Rev Cardiol 11:443–457. https://doi.org/10.1038/nrcardio.2014.80
4. Wolf D, Ley K (2019) Immunity and inflammation in atherosclerosis. Circ Res 124:315–327. https://doi.org/10.1161/CIRCRESAHA.118.313591
5. Libby P, Ridker PM, Hansson GK (2009) Inflammation in atherosclerosis. from pathophysiology to practice. J Am Coll Cardiol 54:2129–2138. https://doi.org/10.1016/j.jacc.2009.09.009
6. Sakakura K, Nakano M, Otsuka F et al (2013) Pathophysiology of atherosclerosis plaque progression. Hear Lung Circ 22:399–411. https://doi.org/10.1016/j.hlc.2013.03.001
7. Alsheikh-Ali AA, Kitsios GD, Balk EM et al (2010) The vulnerable atherosclerotic plaque: scope of the literature. Ann Intern Med 153:387–395. https://doi.org/10.7326/0003-4819-153-6-201009210-00272
8. Schaar JA, De Korte CL, Mastik F et al (2003) Characterizing vulnerable plaque features with intravascular elastography. Circulation 108:2636–2641. https://doi.org/10.1161/01.CIR.0000097067.96619.1F
9. Shah PK, Los Angeles F (2003) Mechanisms of plaque vulnerability and rupture. J Am Coll Cardiol 41:S15–S22. https://doi.org/10.1016/S0735-1097
10. Bailey G, Meadows J, Morrison AR (2016) Imaging atherosclerotic plaque calcification: translating biology. Curr Atheroscler Reports 188(18):1–8. https://doi.org/10.1007/S11883-016-0601-6
11. Pugliese G, Iacobini C, Fantauzzi CB, Menini S (2015) The dark and bright side of atherosclerotic calcification. Atherosclerosis 238:220–230. https://doi.org/10.1016/J.ATHEROSCLEROSIS.2014.12.011
12. Almeida SO, Budoff M (2019) Effect of statins on atherosclerotic plaque. Trends Cardiovasc Med 29:451–455. https://doi.org/10.1016/J.TCM.2019.01.001
13. Roth GA, Johnson C, Abajobir A et al (2017) Global, regional, and national burden of cardiovascular diseases for 10 causes, 1990 to 2015. J Am Coll Cardiol 70:1–25. https://doi.org/10.1016/j.jacc.2017.04.052
14. Brown MS, Goldstein JL (2006) Lowering LDL—not only how low, but how long? Science (80-) 311:1721–1723. https://doi.org/10.1126/science.1125884
15. Brown BG, Zhao XQ, Sacco DE, Albers JJ (1993) Lipid lowering and plaque regression: new insights into prevention of plaque disruption and clinical events in coronary disease. Circulation 87:1781–1791. https://doi.org/10.1161/01.cir.87.6.1781
16. Nissen SE, Nicholls SJ, Sipahi I et al (2006) Effect of very high-intensity statin therapy on regression of coronary atherosclerosis: the ASTEROID trial. J Am Med Assoc 295:1556–1565. https://doi.org/10.1001/jama.295.13.jpc60002
17. Björkegren JLM, Hägg S, Talukdar HA et al (2014) Plasma cholesterol-induced lesion networks activated before regression of early, mature, and advanced atherosclerosis. PLoS Genet. https://doi.org/10.1371/journal.pgen.1004201

18. Giachelli CM (2004) Vascular calcification mechanisms. J Am Soc Nephrol 15:2959–2964. https://doi.org/10.1097/01.ASN.0000145894.57533.C4

19. Vengrenyuk Y, Carlier S, Xanthos S et al (2006) A hypothesis for vulnerable plaque rupture due to stress-induced debonding around cellular microcalcifications in thin fibrous caps. Proc Natl Acad Sci U S A 103:14678–14683. https://doi.org/10.1073/pnas.0606310103

20. Høilund-Carlsen PF, Moghbel MC, Gerke O, Alavi A (2019) Evolving role of PET in detecting and characterizing atherosclerosis. PET Clin 14:197–209. https://doi.org/10.1016/j.cpet.2018.12.001

21. Agatston AS, Janowitz WR, Hildner FJ et al (1990) Quantification of coronary artery calcium using ultrafast computed tomography. J Am Coll Cardiol 15:827–832. https://doi.org/10.1016/0735-1097(90)90282-T

22. Osborn EA, Jaffer FA (2013) Imaging atherosclerosis and risk of plaque rupture. Curr Atheroscler Rep. https://doi.org/10.1007/s11883-013-0359-z

23. Fiz F, Morbelli S, Piccardo A et al (2015) 18F-NaF uptake by atherosclerotic plaque on PET/CT imaging: Inverse correlation between calcification density and mineral metabolic activity. J Nucl Med 56:1019–1023. https://doi.org/10.2967/jnumed.115.154229

24. Voros S, Rinehart S, Qian Z et al (2011) Prospective validation of standardized, 3-dimensional, quantitative coronary computed tomographic plaque measurements using radiofrequency backscatter intravascular ultrasound as reference standard in intermediate coronary arterial lesions. JACC Cardiovasc Interv 4:198–208. https://doi.org/10.1016/j.jcin.2010.10.008

25. McKenney-Drake ML, Moghbel MC, Paydary K et al (2018) 18F-NaF and 18F-FDG as molecular probes in the evaluation of atherosclerosis. Eur J Nucl Med Mol Imaging 45:2190–2200. https://doi.org/10.1007/s00259-018-4078-0

26. Seraj SM, Raynor WY, Revheim ME et al (2020) Assessing the feasibility of NaF-PET/CT versus FDG-PET/CT to detect abdominal aortic calcification or inflammation in rheumatoid arthritis patients. Ann Nucl Med 34:424–431. https://doi.org/10.1007/s12149-020-01463-w

27. Høilund-Carlsen PF, Edenbrandt L, Alavi A (2019) Global disease score (GDS) is the name of the game! Eur J Nucl Med Mol Imaging 46:1768–1772. https://doi.org/10.1007/s00259-019-04383-8

28. Chen W, Dilsizian V (2015) PET assessment of vascular inflammation and atherosclerotic plaques: SUV or TBR? J Nucl Med 56:503–504. https://doi.org/10.2967/jnumed.115.154385

29. Slart RHJA, Glaudemans AWJM, Gheysens O et al (2021) Procedural recommendations of cardiac PET/CT imaging: standardization in inflammatory-, infective-, infiltrative-, and innervation (4Is)-related cardiovascular diseases: a joint collaboration of the EACVI and the EANM. Eur J Nucl Med Mol Imaging 48:1016–1039

30. Oh M, Kim JY, Shin KH et al (2010) (2010) Imaging Atherosclerosis in the carotid arteries with F-18-fluoro-2-deoxy-D-glucose positron emission tomography: effect of imaging time after injection on quantitative measurement. Nucl Med Mol Imaging 44:261–266. https://doi.org/10.1007/S13139-010-0043-Y

31. Derlin T, Habermann CR, Hahne JD et al (2011) Quantification of [18F]-FDG uptake in atherosclerotic plaque: impact of renal function. Ann Nucl Med 25:586–591. https://doi.org/10.1007/S12149-011-0503-1

32. Johnsrud K, Seierstad T, Russell D, Revheim M-E (2020) Inter-reader agreement of 18F-FDG PET/CT for the quantification of carotid artery plaque inflammation. JRSM Cardiovasc Dis 9:204800402098094. https://doi.org/10.1177/2048004020980941

33. Høilund-Carlsen PF, Piri R, Gerke O et al (2021) Assessment of total-body atherosclerosis by PET/computed tomography. PET Clin 16:119–128. https://doi.org/10.1016/j.cpet.2020.09.013

34. Raynor WY, Sang Uk Park P, Borja AJ et al (2021) PET-BASED imaging with 18F-FDG and 18F-NaF to assess inflammation and microcalcification in atherosclerosis and other vascular and thrombotic disorders. Diagnostics 11:2234. https://doi.org/10.3390/DIAGNOSTICS11122234

35. Saboury B, Edenbrandt L, Piri R et al (2021) Alavi-Carlsen calcification score (ACCS): a simple measure of global cardiac atherosclerosis burden. Diagnostics 11:1421. https://doi.org/10.3390/DIAGNOSTICS11081421

36. Arani LS, Zirakchian Zadeh M, Saboury B et al (2021) Assessment of atherosclerosis in multiple myeloma and smoldering myeloma patients using 18F- sodium fluoride PET/CT. J Nucl Cardiol. https://doi.org/10.1007/s12350-020-02446-0

37. Takx RAP, van Asperen R, Bartstra JW et al (2020) Determinants of 18F-NaF uptake in femoral arteries in patients with type 2 diabetes mellitus. J Nucl Cardiol. https://doi.org/10.1007/s12350-020-02099-z

38. Sorci O, Batzdorf AS, Mayer M et al (2020) 18 F-sodium fluoride PET/CT provides prognostic clarity compared to calcium and Framingham risk scoring when addressing whole-heart arterial calcification. Eur J Nucl Med Mol Imaging 47:1678–1687. https://doi.org/10.1007/S00259-019-04590-3

39. Deichen JT, Prante O, Gack M et al (2003) Uptake of [18F]fluorodeoxyglucose in human monocyte-macrophages in vitro. Eur J Nucl Med Mol Imaging 30:267–273. https://doi.org/10.1007/s00259-002-1018-8

40. Ogawa M, Nakamura S, Saito Y et al (2012) What can be seen by 18F-FDG PET in atherosclerosis imaging? The effect of foam cell formation on 18F-FDG uptake to macrophages in vitro. J Nucl Med 53:55–58. https://doi.org/10.2967/jnumed.111.092866

41. Robbie L, Libby P (2001) Inflammation and atherothrombosis. Ann N Y Acad Sci 947:167–180. https://doi.org/10.1111/j.1749-6632.2001.tb03939.x

42. Van Der Wal AC, Becker AE, Van Der Loos CM, Das PK (1994) Site of intimal rupture or erosion of thrombosed coronary atherosclerotic plaques is characterized by an inflammatory process irrespective of the dominant plaque morphology. Circulation 89:36–44. https://doi.org/10.1161/01.CIR.89.1.36

43. Ogawa M, Ishino S, Mukai T et al (2004) 18F-FDG accumulation in atherosclerotic plaques: Immunohistochemical and PET imaging study. J Nucl Med 45:1245–1250

44. Hansson GK, Libby P, Tabas I (2015) Inflammation and plaque vulnerability. J Intern Med 278:483–493. https://doi.org/10.1111/joim.12406

45. Yun M, Jang S, Cucchiara A et al (2002) 18F FDG uptake in the large arteries: a correlation study with the atherogenic risk factors. Semin Nucl Med 32:70–76. https://doi.org/10.1053/snuc.2002.29279

46. Tatsumi M, Cohade C, Nakamoto Y, Wahl RL (2003) Fluorodeoxyglucose uptake in the aortic wall at PET/CT: possible finding for active atherosclerosis. Radiology 229:831–837. https://doi.org/10.1148/radiol.2293021168

47. Bural GG, Torigian DA, Chamroonrat W et al (2008) FDG-PET is an effective imaging modality to detect and quantify age-related atherosclerosis in large arteries. Eur J Nucl Med Mol Imaging 35:562–569. https://doi.org/10.1007/s00259-007-0528-9

48. Tahara N, Kai H, Yamagishi S, Mizoguchi M et al (2007) Vascular inflammation evaluated by [18F]-Fluorodeoxyglucose positron emission tomography is associated with the metabolic syndrome. J Am Coll Cardiol 49:1533–1539. https://doi.org/10.1016/j.jacc.2006.11.046

49. Wassélius J, Larsson S, Sundin A, Jacobsson H (2009) Assessment of inactive, active and mixed atherosclerotic plaques by 18F-FDG-PET; an age group-based correlation with cardiovascular risk factors. Int J Cardiovasc Imaging 25:133–140. https://doi.org/10.1007/s10554-008-9366-5

50. Paulmier B, Duet M, Khayat R et al (2008) Arterial wall uptake of fluorodeoxyglucose on PET imaging in stable cancer disease patients indicates higher risk for cardiovascular events. J Nucl Cardiol 15:209–217. https://doi.org/10.1016/j.nuclcard.2007.10.009

51. Ben-Haim S, Kupzov E, Tamir A, Israel O (2004) Evaluation of18F-FDG uptake and arterial wall calcifications using18F-FDG PET/CT. J Nucl Med 45:1816–1821

52. Dunphy MPS, Freiman A, Larson SM, Strauss HW (2005) Association of vascular 18F-FDG uptake with vascular calcification. J Nucl Med 46:1278–1284

53. Blau M, Ganatra R, Bender MA (1972) 18F-fluoride for bone imaging. Semin Nucl Med 2:31–37. https://doi.org/10.1016/S0001-2998(72)80005-9

54. Kulshrestha RK, Vinjamuri S, England A et al (2016) The role of 18F-sodium fluoride PET/CT bone scans in the diagnosis of metastatic bone disease from breast and prostate cancer. J Nucl Med Technol 44:217–222. https://doi.org/10.2967/jnmt.116.176859

55. Chen K, Blebea J, Laredo JD et al (2008) Evaluation of musculoskeletal disorders with PET, PET/CT, and PET/MR imaging. PET Clin 3:451–465. https://doi.org/10.1016/j.cpet.2009.03.003

56. Creager MD, Hohl T, Hutcheson JD et al (2019) 18F-fluoride signal amplification identifies microcalcifications associated with atherosclerotic plaque instability in positron emission tomography/computed tomography images. Circ Cardiovasc Imaging 12:7835. https://doi.org/10.1161/CIRCIMAGING.118.007835

57. Høilund-Carlsen PF, Sturek M, Alavi A, Gerke O (2020) Atherosclerosis imaging with 18F-sodium fluoride PET: state-of-the-art review. Eur J Nucl Med Mol Imaging 47:1538–1551. https://doi.org/10.1007/s00259-019-04603-1

58. de Oliveira-Santos M, Castelo-Branco M, Silva R et al (2017) Atherosclerotic plaque metabolism in high cardiovascular risk subjects—a subclinical atherosclerosis imaging study with 18F-NaF PET-CT. Atherosclerosis 260:41–46. https://doi.org/10.1016/j.atherosclerosis.2017.03.014

59. Rojulpote C, Patil S, Gonuguntla K et al (2020) NaF-PET/CT global assessment in detecting and quantifying subclinical cardiac atherosclerosis and its association with blood pressure in non-dyslipidemic individuals. Am J Cardiovasc Dis 10:101–107

60. Zhang V, Borja AJ, Rojulpote C et al (2020) Global quantification of pulmonary artery atherosclerosis using 18F-sodium fluoride PET/CT in at-risk subjects. Am J Nucl Med Mol Imaging 10:119–126

61. Kwiecinski J, Tzolos E, Adamson PD et al (2020) Coronary 18F-sodium fluoride uptake predicts outcomes in patients with coronary artery disease. J Am Coll Cardiol 75:3061–3074. https://doi.org/10.1016/j.jacc.2020.04.046

62. Kitagawa T, Yamamoto H, Nakamoto Y et al (2018) Predictive value of18F-sodium fluoride positron emission tomography in detecting high-risk coronary artery disease in combination with computed tomography. J Am Heart Assoc. https://doi.org/10.1161/JAHA.118.010224

63. Cecelja M, Moore A, Fogelman I et al (2019) Evaluation of aortic 18 F-NaF tracer uptake using PET/CT as a predictor of aortic calcification in postmenopausal women: a longitudinal study. JRSM Cardiovasc Dis 8:204800401984887. https://doi.org/10.1177/2048004019848870

64. Raynor W, Houshmand S, Gholami S et al (2016) Evolving role of molecular imaging with 18F-sodium fluoride PET as a biomarker for calcium metabolism. Curr Osteoporos Rep 14:115–125. https://doi.org/10.1007/s11914-016-0312-5

65. Blake GM, Park-Holohan SJ, Cook GJR, Fogelman I (2001) Quantitative studies of bone with the use of 18F-fluoride and 99mTc-methylene diphosphonate. Semin Nucl Med 31:28–49. https://doi.org/10.1053/snuc.2001.18742

66. Joshi NV, Vesey AT, Williams MC et al (2014) 18F-fluoride positron emission tomography for identification of ruptured and high-risk coronary atherosclerotic plaques: a prospective clinical trial. Lancet 383:705–713. https://doi.org/10.1016/S0140-6736(13)61754-7

67. Arbab-Zadeh A, Fuster V (2015) The myth of the "vulnerable plaque": transitioning from a focus on individual lesions to atherosclerotic disease burden for coronary artery disease risk assessment. J Am Coll Cardiol 65:846–855. https://doi.org/10.1016/j.jacc.2014.11.041

68. Narula J, Nakano M, Virmani R et al (2013) Histopathologic characteristics of atherosclerotic coronary disease and implications of the findings for the invasive and noninvasive detection of vulnerable plaques. J Am Coll Cardiol 61:1041–1051. https://doi.org/10.1016/j.jacc.2012.10.054

69. Raynor WY, Borja AJ, Rojulpote C et al (2020) 18F-sodium fluoride: an emerging tracer to assess active vascular microcalcification. J Nucl Cardiol. https://doi.org/10.1007/s12350-020-02138-9

70. Tarkin JM, Joshi FR, Evans NR et al (2017) Detection of atherosclerotic inflammation by 68Ga-DOTATATE PET compared to [18F]FDG PET imaging. J Am Coll Cardiol 69:1774–1791. https://doi.org/10.1016/j.jacc.2017.01.060

71. Kircher M, Tran-Gia J, Kemmer L et al (2020) Imaging inflammation in atherosclerosis with CXCR4-directed 68Ga-pentixafor PET/CT: correlation with 18F-FDG PET/CT. J Nucl Med 61:751–756. https://doi.org/10.2967/jnumed.119.234484

72. Mateo J, Izquierdo-Garcia D, Badimon JJ et al (2014) Noninvasive assessment of hypoxia in rabbit advanced atherosclerosis using 18f-fluoromisonidazole positron emission tomographic imaging. Circ Cardiovasc Imaging 7:312–320. https://doi.org/10.1161/CIRCIMAGING.113.001084

73. Joseph P, Tawakol A (2016) Imaging atherosclerosis with positron emission tomography. Eur Heart J 37:2974–2980b. https://doi.org/10.1093/eurheartj/ehw147

74. Dilsizian V, Jadvar H (2017) Science to practice: Does FDG differentiate morphologically unstable from stable atherosclerotic plaque? Radiology 283:1–3. https://doi.org/10.1148/radiol.2017162495

75. Brammen L, Palumbo B, Lupattelli G, Sinzinger H (2014) Is 18F-FDG PET really a promising marker for clinically relevant atherosclerosis? Hell J Nucl Med 17:62–63

76. Lodge MA, Rahmim A, Wahl RL (2009) A practical, automated quality assurance method for measuring spatial resolution in PET. J Nucl Med 50:1307–1314. https://doi.org/10.2967/jnumed.108.060079

77. Zaidi H, Alavi A (2007) Current trends in PET and combined (PET/CT and PET/MR) systems design. PET Clin 2:109–123. https://doi.org/10.1016/j.cpet.2007.10.004

78. Rousset O, Rahmim A, Alavi A, Zaidi H (2007) Partial Volume Correction Strategies in PET. PET Clin 2:235–249. https://doi.org/10.1016/j.cpet.2007.10.005

79. Blomberg BA, de Jong PA, Thomassen A et al (2017) Thoracic aorta calcification but not inflammation is associated with increased cardiovascular disease risk: results of the CAMONA study. Eur J Nucl Med Mol Imaging 44:249–258. https://doi.org/10.1007/s00259-016-3552-9

80. Dweck MR, Chow MWL, Joshi NV et al (2012) Coronary arterial 18F-sodium fluoride uptake: a novel marker of plaque biology. J Am Coll Cardiol 59:1539–1548. https://doi.org/10.1016/j.jacc.2011.12.037

81. Alavi A, Werner TJ, Høilund-Carlsen PF (2018) What can be and what cannot be accomplished with PET to detect and characterize

atherosclerotic plaques. J Nucl Cardiol 25:2012–2015. https://doi.org/10.1007/s12350-017-0977-x